11th International Conference on Fracture Mechanics of Concrete and Concrete Structures
FraMCoS-11
J. M. Chandra Kishen, A. Ramaswamy, S. Ray and R. Vidyasagar (Eds)
https://doi.org/10.21012/FC11.092358

NON-DESTRUCTIVE DETECTION OF AN ARTIFICIAL DEFECT IN CONCRETE WITH INFRARED THERMOGRAPHY AND HEAT BALANCE SIMULATION

TAIKI HAGIWARA[*], YUMA SHIMAMOTO[**] AND TETSUYA SUZUKI[***]

[*] Graduate School of Science and Technology, Niigata University
8050 2-no-cho, Ikarashi, Nishi-ku, Niigata-shi, Niigata 950-2181, Japan
e-mail: f21n001c@mail.cc.niigata-u.ac.jp, www.gs.niigata-u.ac.jp

[**] Institute of Agriculture, Tokyo University of Agriculture and Technology
3-5-8 Saiwai-cho, Fuchu-shi, Tokyo 183-8509, Japan
e-mail: simamoto@go.tuat.ac.jp, www.tuat.ac.jp

[***] Faculty of Agriculture, Niigata University
8050, 2-no-cho, Ikarashi, Nishi-ku, Niigata-shi, Niigata 950-2181, Japan
e-mail: suzuki@agr.niigata-u.ac.jp, www.agr.niigata-u.ac.jp

Key words: Non-destructive test, Defect detection, Heat balance simulation, Infrared thermography

Abstract: Infrared thermography is used to detect the differences of temperature fields between concrete with inner defects and without defects. The accuracy of the inspection for on-site monitoring is affected by weather conditions. This study develops a combination method of infrared thermography and a heat balance simulation based on meteorological data for non-destructive detection of concrete defects. In experimental procedures, two kinds of concrete samples were set to non-defect concrete and artificial defect concrete. These samples were used to conduct a passive test. In analytical procedures, the heat balance simulation calculates concrete surface temperatures from meteorological data. Temperatures inside concrete is obtained from the numerical solution of the one-dimensional heat conduction equation. As a result, The infrared thermography and the heat balance simulation can detect the differences in surface temperatures between non-defect and artificial defect samples.

1 INTRODUCTION

Infrared thermography, which is one of non-destructive tests, efficiently inspects defects of concrete structures from surface temperature fields [1, 2]. Infrared thermography can detect differences of temperature fields between concrete with inner defects and without defects owing to material thermal mass. The accuracy of infrared thermography inspection for on-site monitoring is affected by weather conditions. This study develops a combination method of infrared thermography and a heat balance simulation including weather conditions for non-destructive detection of concrete defects. A heat balance means an energy flux balance. This simulation is often used to calculate water [3, 4] and ground surface temperatures [5] on a macro scale. This study tries to use this idea for calculating concrete surface temperatures. The heat balance simulation estimates the concrete surface temperatures based on weather conditions and thermal characteristics of the material. Using both the thermography and the simulation tries to improve the non-destructive detection of inner defects of concrete.

2 MATERIALS AND METHODS

2.1 Concrete test samples

Two kinds of concrete test samples were set, a non-defect sample (Case 1) and a defect sample (Case 2). The mixture proportions of the test sample are shown in Table 1. The test sample had 150 mm long, width and height. Case 2 had an artificial defect with 70 mm long and width and 10 mm height in the test sample. The artificial defect with expanded polystyrene was in 50 mm depth from the top surface. The faces except the top surface of the test samples were covered with insulation material (expanded polystyrene) to conduct a passive test in 2.2. The exterior of the test sample is shown in Figure 1. Thermocouples were set on the surface and in the inside of the test sample to measure temperatures. The positions of the thermocouples are shown in Figure 2. The thermocouple CH1 was set at the edge of the sample surface because thermal images of the surface were acquired by infrared thermography.

2.2 A passive test

A passive test is one of the infrared thermography tests. The test aims to detect a temperature field, which is generated by unartificial heat transfer, using infrared thermography. In this study, the passive test tried to detect the differences in the temperatures of non-defect and defect samples. The test was conducted at the roof of the Faculty of Agriculture, Niigata University between 31 July and 30 August in 2019. The temperatures of the concrete samples, the temperature fields on the sample surfaces, and meteorological data were measured by thermocouples, an infrared thermography camera (R300SR, Nippon Avionics) and a weather station (HOBO, Onset). The meteorological data included precipitation, air temperature, wind speed and solar radiation data. The setup for the passive test is shown in Figure 3. The thermocouples and weather station acquired the data at 30-minutes intervals. The thermography camera captured thermal images of the sample surface at 1-hour intervals from 5:00 to 19:00.

Table 1: Mixture proportions of concrete test samples

Maximum gravel size	Water to cement ratio	Volume ration of fine aggregate	Slump value	Air content	Weight per unit volume of concrete (kg/m^3)			
(mm)	(%)	(%)	(cm)	(%)	W	C	S	G
25	57	39	8	5	151	253	737	1150

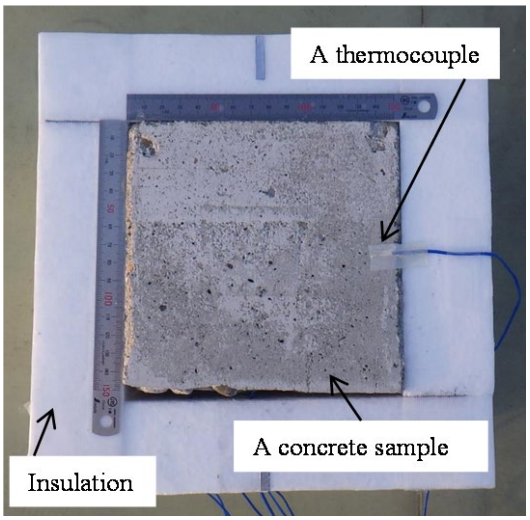

Figure 1: A concrete test sample.

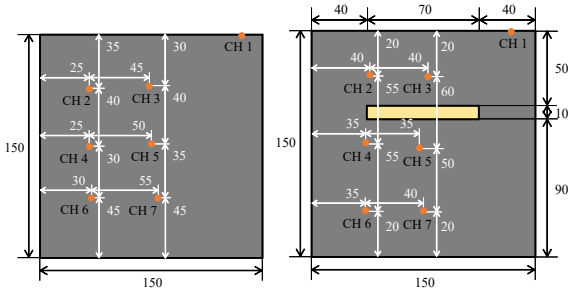

(a) Case 1 (b) Case 2

Figure 2: Positions of thermocouples in depth.

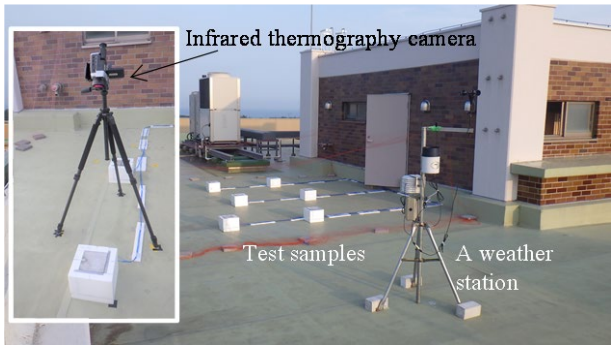

Figure 3: The setup for a passive test.

3 ANALYTICAL PROCEDURES

3.1 Heat balance on concrete surface

In the agrometeorology field, applying a

heat balance on ground surface can calculate the surface temperature, ground temperature and water temperature. The schematic diagram of the heat balance on ground surface is shown in Figure 4. The kinds of solar radiation include direct solar radiation that reaches the ground surface directly from the solar sphere, scattering solar radiation that reaches the ground surface owing to scattering in the atmosphere, and reflecting solar radiation that is reflected from the ground surface. The combination of the direct and scattering solar radiation means global solar radiation. These are shortwave radiation owing to the wavelength range up to 3.0 μm. Infrared radiation originates from greenhouse gases such as water vapor and carbon dioxide in the atmosphere. The ground surface emits infrared radiation corresponding to the ground surface temperature. These are longwave radiation owing to the wavelength range of 3.0 μm or longer. Sensible heat and latent heat are the energy transported by air and water vapor on the ground surface. The energy due to heat conduction to the ground means ground conduction heat.

The idea of the heat balance on the ground surface is applied to the calculation of material surface temperatures. The heat balance on concrete surface is shown in Figure 5. Based on this figure, the simulation model using meteorological data for the heat balance analysis is explained. In this paper, net radiation, sensible heat flux and conductive heat flux inside the concrete sample are considered. The net radiation is the sum of downward solar and atmospheric radiation, and upward reflected solar and infrared radiation. The sensible heat flux is convection flux between the target surface and atmosphere owing to wind. The conductive heat flux is conduction flux inside the concrete sample owing to temperature gradient. R_n is the net radiation (W/m^2), H is the sensible heat flux(W/m^2), and G is the conductive heat flux(W/m^2). The formula of the heat balance is given by Equation (1),

$$R_n = H + G. \quad (1)$$

The net radiation on the left side is expressed in Equation (2),

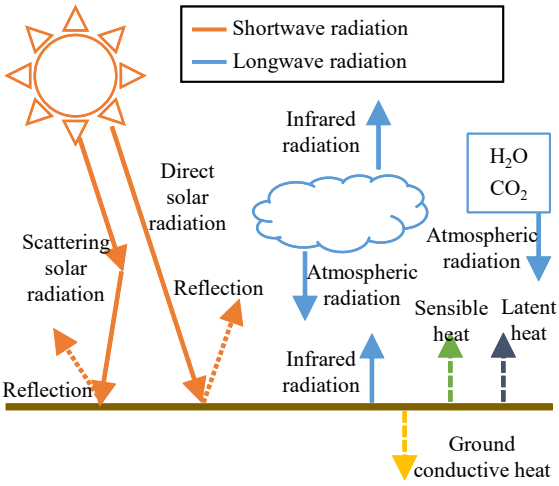

Figure 4: The energy balance on the Earth.

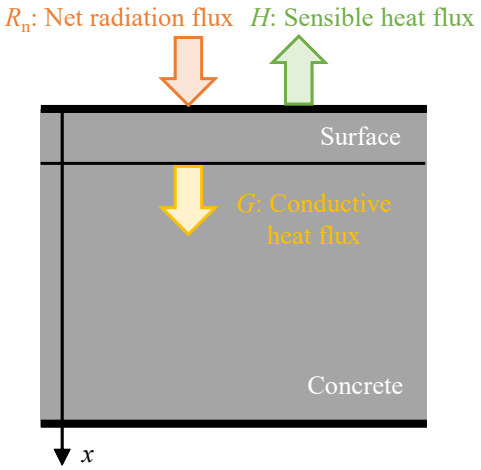

Figure 5: Heat balance on concrete surface.

$$R_n = (1-\alpha)S_d + L_d - \varepsilon\sigma T_s^4, \quad (2)$$

where α is the albedo, S_d is the solar radiation, L_d is the atmospheric radiation, ε is the emissivity, σ is the Stefan-Boltzmann constant (= 5.67×10-8 W/m^2/ K^4), and T_s is the surface temperature of the concrete sample.

The sensible heat flux H in the first term on the right side of Equation (1) is expressed by Equation (3),

$$H = c_a \rho_a C_H U (T_s - T_a), \quad (3)$$

where c_a is the specific heat of air (J/kg/K), ρ_a is the density of air (kg/m^3), C_HU is the exchange speed of the sensible heat flux (m/s), and T_a is the air temperature (K). C_HU depends on the surface characteristics. In this study, concrete surface is assumed to be equal to bare ground, and C_HU is calculated by Equation (4),

$$C_H U = 0.0027 + 0.0031U, \quad (4)$$

where U is the wind speed (m/s).

The conductive heat flux G in the second term on the right side of Equation (1) is expressed by Equation (5),

$$G = \int_0^D \frac{d(c_G \rho_G T_G)}{dt} dx, \quad (5)$$

where c_G is the specific heat of concrete (J/kg/K), ρ_G is the density of concrete (kg/m^3), T_G is the air temperature (K), and D is the depth where the heat conduction is almost zero.

3.2 Analytical conditions

Calculating the heat flux due to the heat balance and heat conduction into the concrete sample needs thermal properties. Analytical conditions of the thermal properties for the simulation are shown in Table 2.

Table 2: Analytical conditions for the simulation

Thermal conductivity (concrete) (W/m/K)	3.0
Specific heat (concrete) (J/kg/K)	1,050
Density (concrete) (kg/m^3)	2,300
Thermal conductivity (air) (W/m/K)	0.0257
Specific heat (air) (J/kg/K)	1007
Density (air) (kg/m^3)	1.166
Emissivity (air) (-)	0.96
Albedo (-)	0.50

4 RESULTS AND DISCUSSION

4.1 Time series of temperatures measured by thermocouples

In chapter 4, the data measured between 1 and 3 August in 2021 are used. Time series of temperatures of the test samples measured by thermocouples are shown in Figure 6. This figure gives the results of only CH 1, 3, 5 and 7 according to the different depth. It is confirmed that the deeper the position, the slower the temperature response and the smaller the temperature change. In Case 2, the differences in the peak temperatures of CH 1 and 3 above the artificial defect and CH 5 and 7 under the one are larger than those in Case 1. This is because the defect in concrete sample blocks the heat conduction. These measured data reveal that the material with the different thermal conductivity (here, air is assumed) in concrete sample varies the heat conduction characteristic.

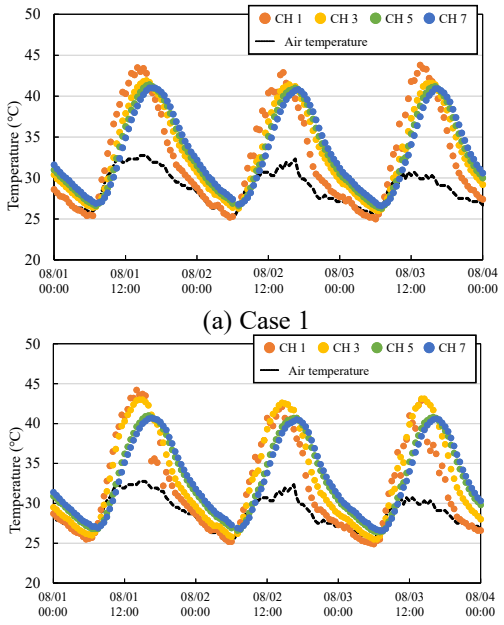

(a) Case 1

(b) Case 2

Figure 6: Time series of temperatures measured by thermocouples.

4.2 The heat balance simulations of the concrete sample temperatures

The results of the heat balance simulations based on meteorological data are shown in Figure 7. The simulated values on the surface correspond to the measured values of CH 1 in the temperature rise process. The measured values are evaluated as temperatures occurring in concrete under weather conditions. The simulation model requires the revision of fitting the temperature drop process.

4.3 The results of infrared thermography

The result of infrared thermography measurements is shown in Figure 8. The temperatures are based on thermal images acquired by the infrared thermography camera. The temperatures of Case 2 in the rise process are higher than those of Case 1, and the

temperatures of Case 2 in the drop process are lower than those of Case 1. From those trends, the effect of the artificial defect on the surface temperatures can be detected using the non-contact method. The heat conduction characteristics with or without the defect in the concrete sample can evaluated in Figure 6. The differences in surface temperatures of non-defect and defect samples are detected considering the inside heat characteristics.

5 CONCLUSIONS

The heat balance simulation enables estimation of the concrete surface temperatures based on weather conditions and thermal characteristics of the material. Using both the thermography and the simulation improve the non-destructive detection of inner defects of concrete.

REFERENCES

[1] Milovanović, B. and Pečur, B., 2016. Review of active IR thermography for detection and characterization of defects in reinforced concrete. *J. of Imaging*. **2**: doi:10.3390/jimaging2020011

[2] Sirca, G.F. and Adeli, H., 2018. Infrared thermography for detecting defects in concrete structures. *J. of Civil Eng. and Mgmt.* **24**: 508-515.

[3] Kimura, M., Kobayashi, S., Mitsuyasu, M., Xie, W. and Iida, T., 2022. Simulation model of water temperature variation in dual-purpose canals considering return flow from up-stream paddy fields. *Irrig. and Drain*. **71**: 138-154.

[4] Maruyama, A., Nemoto, M., Hamasaki, T., Ishida, S. and Kuwagata, T., 2017. A water temperature simulation model for rice paddies with variable water depths, *Water Resour. Res*. 53: 10065-10084.

[5] Kondo, J., 1992. Application of analytical solution to the ground surface temperature and heat flux estimation, *J. Agr. Met*. 48: 265-275.

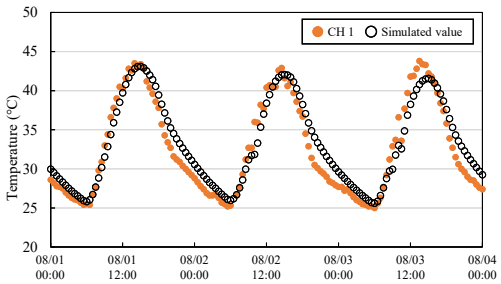

(a) Case 1

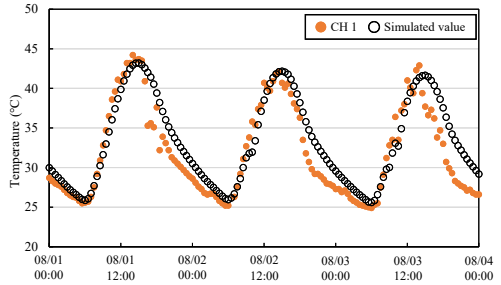

(b) Case 2

Figure 7: The comparison of measured and simulated temperatures on concrete surface.

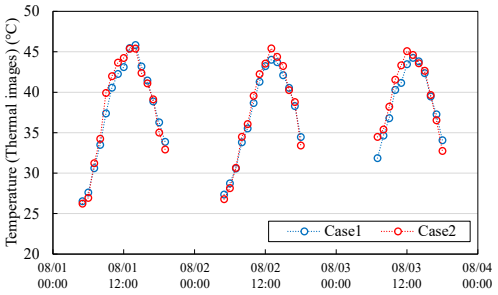

Figure 8: The comparison of temperatures by thermal images of Case 1 and 2.